

# Assessment of Using GNSS for the Monitoring of the Atmospheric Water Vapour Content Over Long Time Scales

Gunnar Elgered<sup>(1)</sup>, Tobias Nilsson<sup>(1)</sup>, Ulrika Willén<sup>(2)</sup>

<sup>(1)</sup> *Department of Radio and Space Science, Chalmers University of Technology,  
Onsala Space Observatory, SE-439 92 Onsala, Sweden  
Email: Gunnar.Elgered@chalmers.se  
Email: Tobias.Nilsson@chalmers.se*

<sup>(2)</sup> *Rosby Centre, Swedish Meteorological and Hydrological Institute,  
SE-601 76 Norrköping, Sweden  
Email: Ulrika.Willen@smhi.se*

## INTRODUCTION

Water vapour in the atmosphere is a parameter of great importance in climate models because of its role as a greenhouse gas. In fact water vapour is a very efficient greenhouse gas. An increase of 20% of the water vapour content in the tropics has a larger impact than a doubling of the carbon dioxide concentration [1]. In this presentation we will focus on the Integrated Precipitable Water Vapour (IPWV), which is measured as the height of the column formed if all the water vapour is condensed and collected at the ground surface, i.e., an IPWV value of 1 mm is equivalent to a water vapour content of 1 kg/m<sup>2</sup>.

Global Navigation Satellite Systems (GNSS) can be used as a tool to estimate the IPWV in the atmosphere. Most of the studies carried out so far have used observations from the Global Positioning System (GPS), see, e.g. [2, 3, 4, 5]. Today there are many national and international GPS networks that have been operating for more than 10 years. The amount of water vapour in the atmosphere has a strong dependence on the temperature which means that water vapour may also be used as a probe for an indirect monitoring of the temperature. Monitoring of the atmospheric water vapour content requires first of all a long term stability. An uncertainty in the absolute value is of less importance, as long as it is stable and can be treated as true offset during the entire study period.

The Total Solar Irradiance (TSI) is another parameter of great importance in climate models. An example with satellite measurements of the TSI is shown in Fig. 1 which clearly illustrates the difference between absolute accuracy and long term stability. It may be worth to note that whereas TSI measurements are measuring emission from the sun, GNSS measurements of the IPWV is based on measurements of differences in time of arrival of radio signals. The latter being a physical quantity which often is more attractive to monitor over long time scales in terms of stability.

We will in the following first summarize the background theory. Thereafter, we show examples of IPWV estimates from GPS data, using the last 10 years of observations in Sweden and Finland and discuss the estimation of linear trends and their uncertainties. Finally we compare the GPS results with the corresponding output from climate models.

## THEORETICAL BACKGROUND

The atmospheric parameter estimated in the GPS data processing is the equivalent excess propagation path referred to the zenith direction, often called the Zenith Total Delay (ZTD). It is often expressed in units of length, using the speed of light in vacuum for the conversion from a time delay. The ZTD can be divided into a Zenith Hydrostatic Delay (ZHD),  $\ell_h$ , and a Zenith Wet Delay (ZWD),  $\ell_w$  [7]

$$\ell_t = \ell_h + \ell_w \quad (1)$$

The hydrostatic term can be determined with an uncertainty of less than 1 mm in the zenith direction if the total ground pressure is measured with an uncertainty of less than 0.5 hPa given that a pressure change of 1 hPa corresponds to a change in the delay of 2.3 mm [7]. The ZWD can be written as [8]

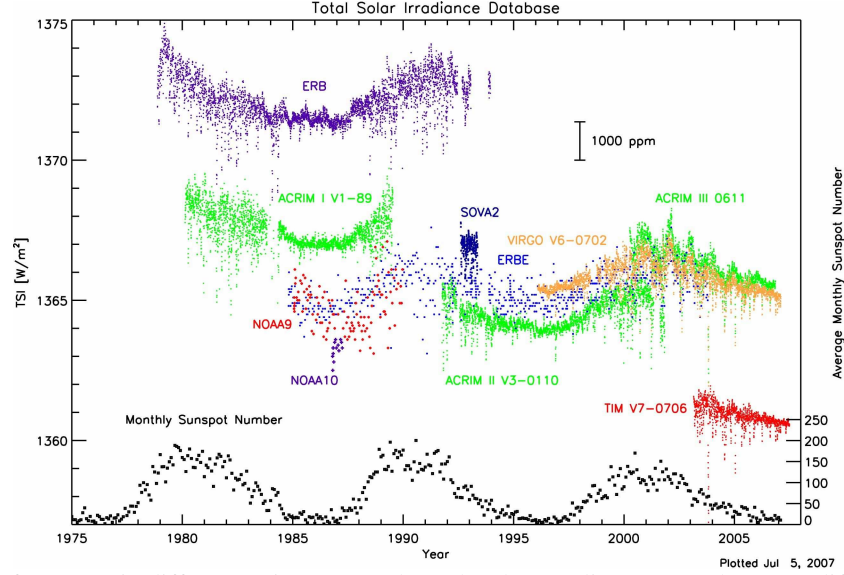


Fig. 1. Illustration of systematic differences in measured Total Solar Irradiance (TSI) between different satellite instruments. Reproduced with permission from G. Kopp, <http://spot.colorado.edu/~kopp/TSI/> (see also [6]).

$$\ell_w = 24 \cdot 10^{-6} \int_0^{\infty} \frac{e(h)}{T(h)} dh + 0.3754 \int_0^{\infty} \frac{e(h)}{T(h)^2} dh \quad [\text{m}] \quad (2)$$

where  $e(h)$  is the profile of the partial pressure of water vapour and  $T(h)$  is the temperature profile, expressed in hPa and K, respectively. The expression for the IPWV is similar:

$$V = \frac{1}{\rho_w} \int_0^{\infty} \rho_v(h) dh \quad (3)$$

where  $\rho_v(h)$  is the density profile of water vapour and  $\rho_w$  is the density of liquid water. The ZWD is closely related to the IPWV because  $\rho_v$  is proportional to  $e/T$ . A conversion factor can be calculated by assuming a value of the mean temperature of the wet refractivity in the atmosphere. This conversion factor can be modelled, e.g., using a history of radiosonde data [9], or calculated using re-analysis data from a numerical weather model such as the ECMWF model [10]. These studies have shown that the IPWV can be estimated from the ZWD with a typical root-mean square (RMS) conversion error of less than 2%.

## ANALYSIS OF GPS DATA FROM SWEPOS AND FINNREF

We have used data from GPS receiver sites in Sweden and Finland. The sites are of geodetic quality, meaning that they are mounted on solid bedrock. Most of the Swedish sites have been in continuous operation since late 1993 and the Finnish sites have been operational since late 1996. Fig. 2 shows these sites in the Swedish SWEPOS network and the Finnish FinnRef network.

The GPS data have been analysed using the GAMIT GPS processing software, developed at the Massachusetts Institute of Technology [11]. The software is based on a method referred to as a network solution. This means that many stations are processed together. In our case all SWEPOS stations are processed in one solution and all FinnRef stations in another. Some of the SWEPOS sites have also been included in the FinnRef solution in order to be able to compare the two solutions. All observations are included down to an elevation cut-off angle of 10 degrees and the elevation dependences of the ZHD and the ZWD were modelled using the mapping functions developed by Niell [12]. In the analysis we estimate station coordinates, satellite coordinates, and the ZTD.

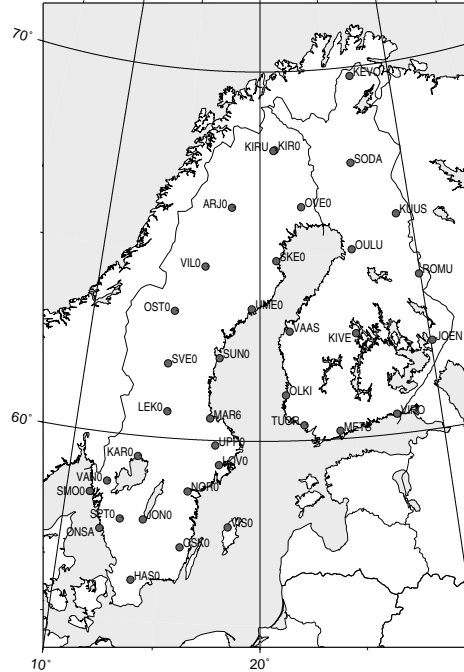


Fig. 2. GPS receiver sites in Sweden and Finland.

### ON THE ESTIMATION OF LINEAR TRENDS IN THE IPWV

In order to obtain the ZWD from the estimated ZTD we use the total pressure at the GPS antenna to calculate and subtract the ZHD. A pressure error of 1 hPa results in an error of 2.3 mm in the ZHD, and hence also in the ZWD. A 2.3 mm error in the ZWD implies an IPWV error of 0.35 mm. The pressure data may be obtained from measurements or modelling work. Since most of the GPS sites do not have any pressure observations it is of interest to assess how well the ground pressure can be modelled. We have compared pressure estimates derived from a model used by the Swedish Meteorological and Hydrological Institute (SMHI) and pressure measurements at the Onsala station (ONSA). The differences between the two time series are shown in Fig. 3(a). They agree with an RMS difference of 0.5 hPa. The observed trend in the difference is  $-0.011$  hPa/year which introduce an error in the IPWV trend of  $-0.004$  mm/year. This drift can be due to a slowly changing error in the barometer or a systematic effect in the model. It is not of great importance here because it is significantly below the uncertainties in the linear trends estimated from the GPS data, as we will show below.

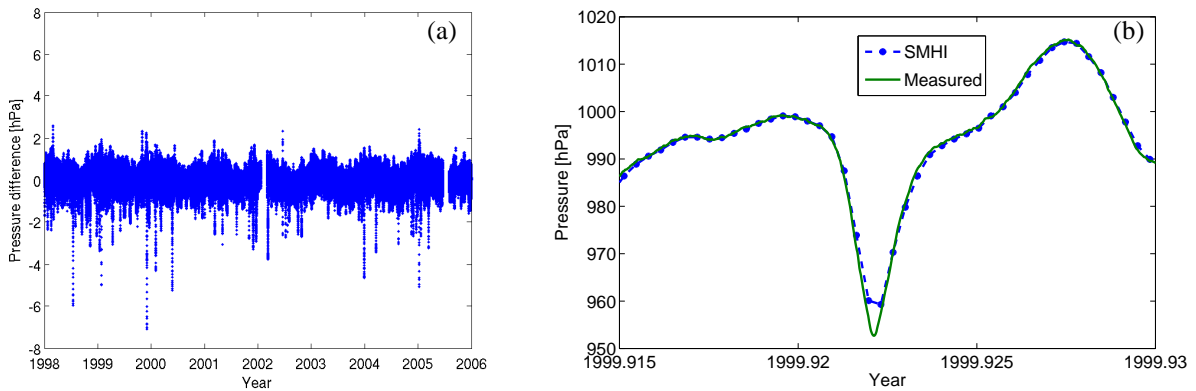


Fig. 3. Comparison between modelled and measured pressure at the Onsala site. The differences (a) are occasionally large due to the 3 h temporal resolution of the model. The largest difference (b) is caused by rapid variations during the passage of a low pressure weather system.

The next conversion, from ZWD to IPWV can also introduce an error in the trend estimates through an unmodelled trend in the conversion factor. This whole problem can of course be avoided if ZWD is analyzed in terms of trends rather than the IPWV. In this work, however, we have done the conversion to IPWV using Equation (3) in [3]

When the IPWV time series have been calculated we use these to estimate the parameters in the following model for each site:

$$V = V_0 + a_1 t + a_2 \sin(2\pi t) + a_3 \cos(2\pi t) + a_4 \sin(4\pi t) + a_5 \cos(4\pi t) \quad (4)$$

where  $t$  is the time in years and the coefficients  $V_0$ ,  $a_1$ ,  $a_2$ ,  $a_3$ ,  $a_4$ , and  $a_5$ , are estimated using the method of least squares. Based on the Lomb-Scargle periodograms [13] we chose to include both annual and semi-annual terms in order to describe the seasonal variations. Two examples are shown in Fig. 4. We note that the semi-annual term is relatively stronger at the Arjeplog site, in the north of Sweden, compared to the results for the Hässleholm site in the south. The original time series and fitted models are presented in Fig. 5.

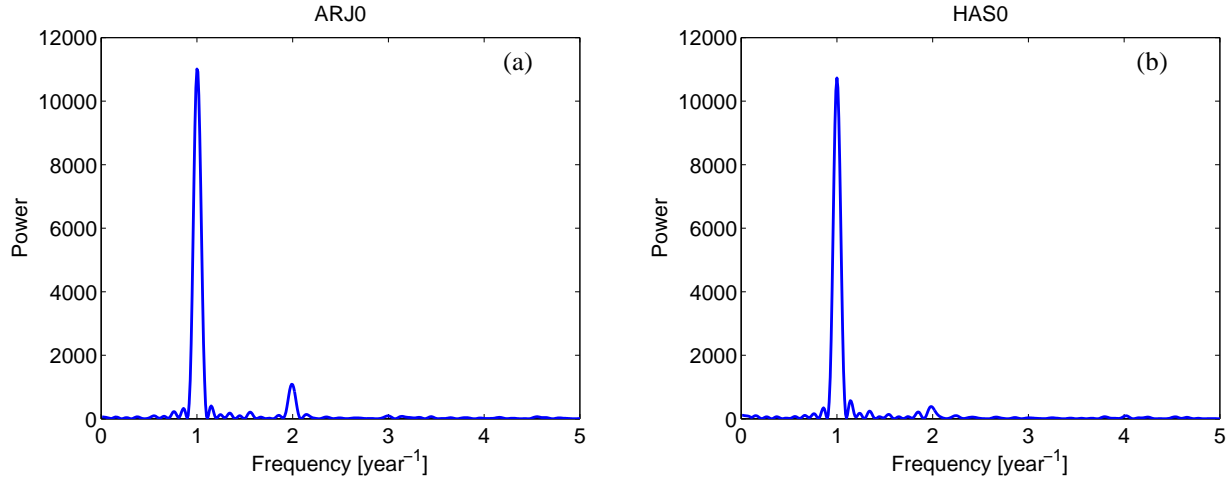


Fig. 4. Lomb-Scargle periodograms for the IPWV time series from (a) Arjeplog and (b) Hässleholm.

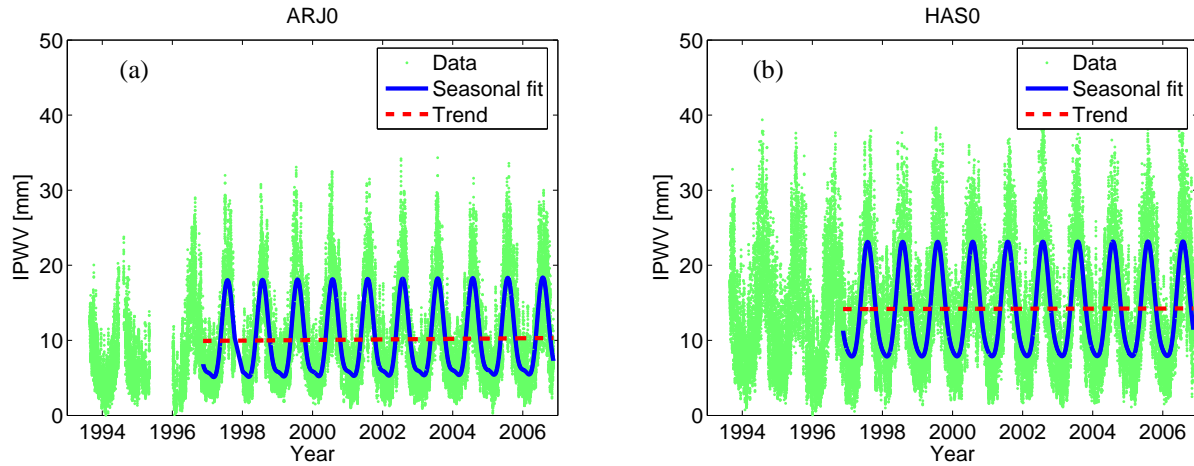


Fig. 5. IPWV time series from (a) Arjeplog and (b) Hässleholm. The straight line is the fitted linear drift and the periodic function models the seasonal variability in accordance with Equation (4).

We have estimated trends for the different sites shown in Fig. 2. We chose to use the data from the time period Nov. 16, 1996 – Nov. 15, 2006. The data acquired with the Swedish network from the first three years (before Nov. 16, 1996) were not used in these estimates of model parameters in order to cover the same time period with all sites. Furthermore, there were a number of radome changes during 1993–1996 which we have earlier shown have a significant impact on the absolute values of the IPWV when performing network solutions [14]. For these ten years the linear trends in the IPWV falls in the range from  $-0.05$  to  $+0.10$  mm/yr. These trends can double if we chose to use data from summer or winter seasons only. They also change significantly if two years of data are ignored in the beginning or in the end of the time series. These results confirm that the variability in the weather from one year to another is large and also confirm that it is reasonable to form mean values over as long time periods as 30 years when characterizing the climate.

The formal uncertainties in the linear trends can be estimated by statistical methods. If we (incorrectly) assume that the deviations from the models are well described by white noise, we obtain one-sigma uncertainties of less than 0.01 mm/yr. The covariances for the deviation can, however, be modelled. We have fitted the following model to the observed covariances between IPWV values  $V_1$  and  $V_2$  observed at the time epochs  $t_1$  and  $t_2$ :

$$\text{Cov}[V_1(t_1), V_2(t_2)] = a_1 2^{-|t_1-t_2|/T_1} + a_2 2^{-|t_1-t_2|/T_2} \quad (5)$$

Fig. 6 shows both the observed data as well as the model fits for the two sites Umeå and Hässleholm. Also shown in these plots is the model result obtained if only one term is used in the covariance model. When taking these covariances into account the formal one-sigma error is approximately 0.04 mm/yr for the ten year data set.

As the time series of GPS data will get longer these formal uncertainties will of course be smaller. At the same time systematic effects will become relatively more important. Potential candidate error sources to be further investigated when using GNSS/GPS data are:

- Elevation cut-off angles influence the atmospheric estimates since phase delay effects introduced by the interaction with the electromagnetic environment at the site are not correctly modelled. Errors in the mapping functions used to describe the elevation dependence of the ZHD and ZWD will also add different bias-type effects depending on the elevation cut-off angle.
- Systematic changes in the satellite constellation over time will change the distribution of observations on the sky and thereby enhance mismodelled phase delay effects of the antennas on the satellites and on the ground.
- Phase patterns of satellite antennas will have systematic impacts on the atmospheric estimates. Especially important is that the net effect will vary with time as one type of satellites is replaced by another [15].

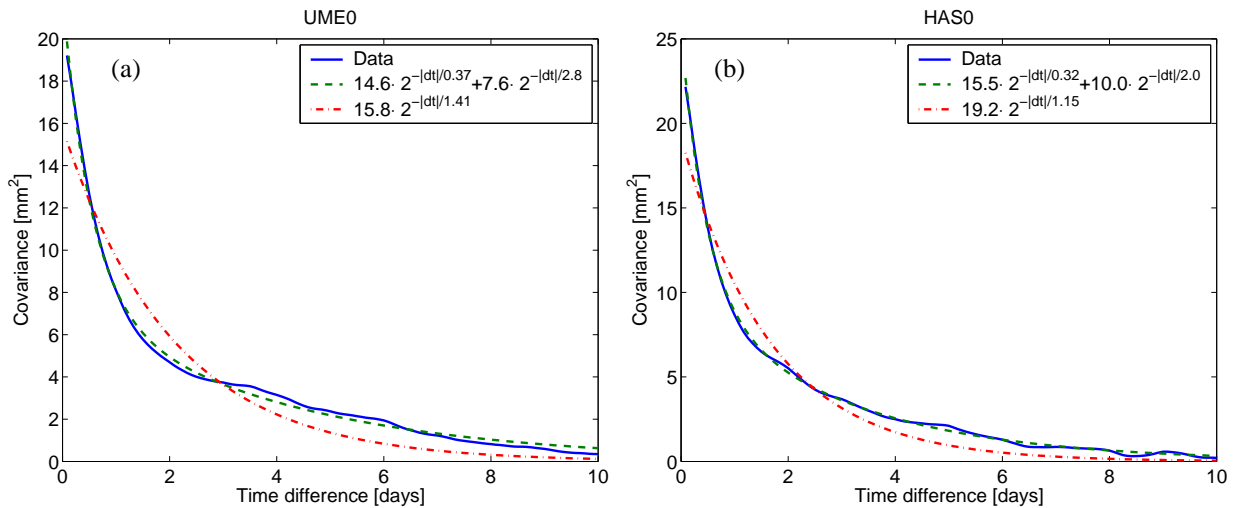


Fig. 6. IPWV time series from (a) Umeå and (b) Hässleholm. The solid line is the observed covariance. The dash-dotted and the dotted lines are the one and the two term models, respectively.

## COMPARISON BETWEEN GPS AND CLIMATE MODEL RESULTS

We have compared two versions of the Rossby Centre Atmospheric regional climate model, RCA2 [16] and RCA3 [17], and the ECMWF Re-Analysis, ERA-40 [18], with the GPS data for five years from 1997 until 2001. Fig. 7 shows the results from the Kiruna site in the north of Sweden. It is clear that the agreement between the GPS data and ERA-40 is better since the ECMWF model was run with data assimilation using observations, while RCA was run in climate mode, i.e. using ERA-40 data at the boundaries and no data assimilation in the interior region.

Another interesting feature is the increasing positive bias of the two RCA models occurring in the summer. Fig. 8 shows the corresponding results for the Visby site on the island of Gotland in the southeast of Sweden. Here there are also some biases of the RCA models in the summer, but not at all as clear as for the Kiruna site. In the future we will continue with these kind of comparisons with the goal to identify systematic differences which in turn, hopefully, can be used to improve the climate models.

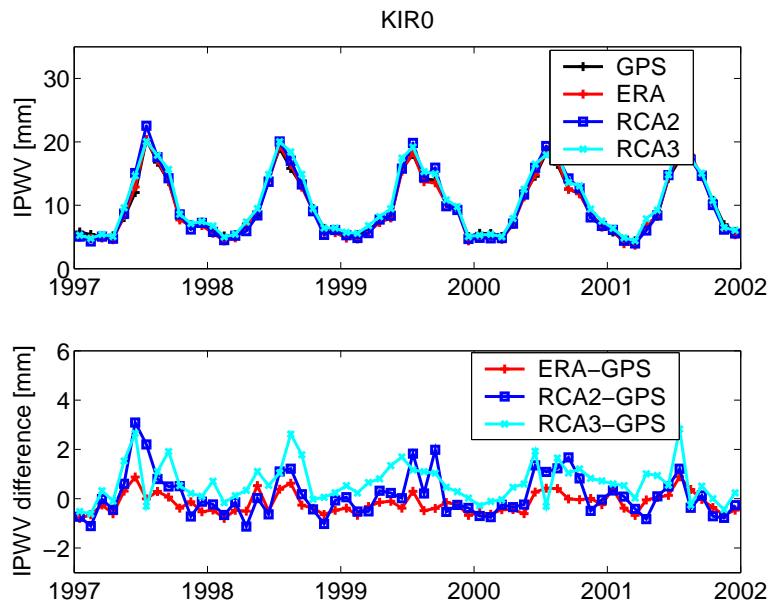


Fig. 7. Time series of the IPWV at the Kiruna site estimated from GPS data and inferred from climate models.

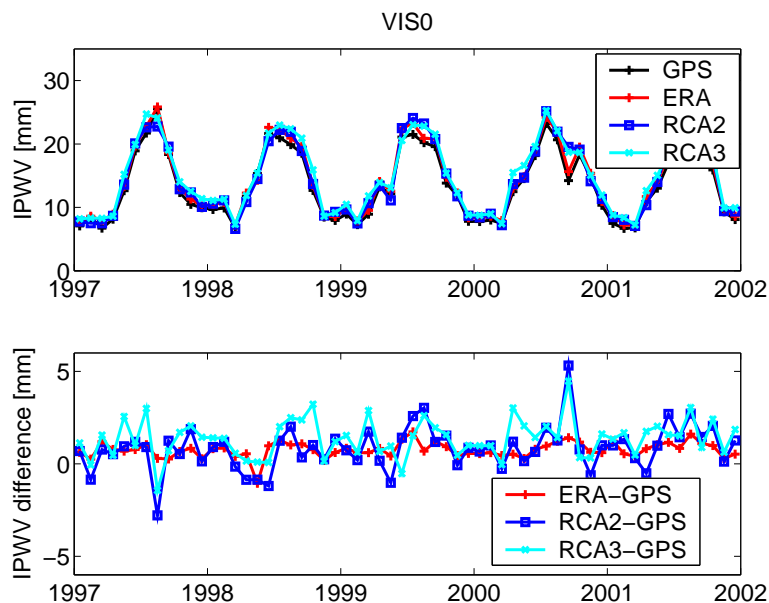


Fig. 8. Time series of the IPWV at the Visby site estimated from GPS data and inferred from climate models.

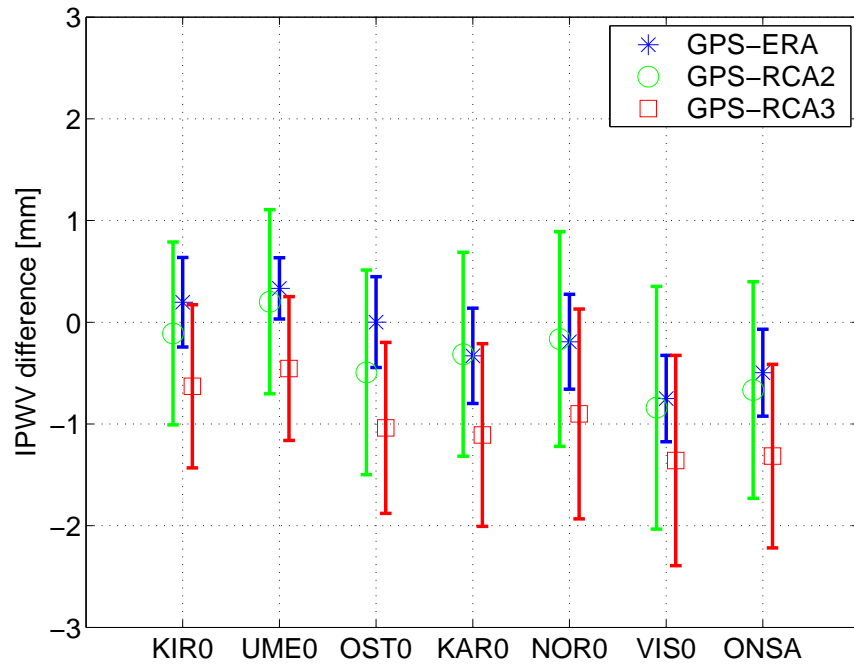


Fig. 9. Mean difference between GPS derived IPWV with the results from the ERA and the RCA models, for Kiruna (KIRO), Umeå (UME0), Östersund (OST0), Karlstad (KAR0), Norrköping (NOR0), Visby (VIS0), and Onsala (ONSA). The errorbars indicate the RMS scatter around the average.

Fig. 9 shows the mean difference (bias) and the RMS scatter between the GPS derived IPWV with the IPWV from ERA40 and the two RCA model versions, for a few selected stations. As expected both the bias and the RMS scatter of the differences around the bias are smaller for the GPS-ERA40 comparison. Studying the two RCA model versions we see that in general there are larger differences at the southern stations, which could be due to higher values of the IPWV in the south. The RCA3 model has a larger bias but a slightly lower RMS compared to the RCA2. This is in agreement with other investigations which indicate that RCA3 overestimates cloud water and IPWV [19]. Further investigations using longer time series and including sites in a larger area are planned for the next couple of years.

**ACKNOWLEDGEMENTS.** We are grateful to Martin Lidberg at Chalmers and Lars Mueller at the SMHI for providing the ZTD time series and the ground meteorological data, respectively. The ongoing research project *Long Term Water Vapour Measurements Using GPS for Improvement of Climate Modelling* is funded by VINNOVA—the Swedish Governmental Agency for Innovation Systems.

## REFERENCES

- [1] S. A. Buehler, A. von Engel, E. Brocard, V. O. John, T. Kuhn, and P. Eriksson, "Recent developments in the line-by-line modeling of outgoing longwave radiation," *JQSRT*, vol. 98, no. 3, pp. 446–457, 2006.
- [2] M. Bevis, S. Businger, T. Herring, C. Rocken, R. Anthes, and R. Ware, "GPS meteorology: Remote sensing of atmospheric water vapor using the Global Positioning System," *J. Geophys. Res.*, vol. 97, pp. 15,787–15,801, 1992.
- [3] T. R. Emardson, G. Elgered, and J. M. Johansson, "Three months of continuous monitoring of atmospheric water vapour with a network of Global Positioning System receivers," *J. Geophys. Res.*, vol. 103, pp. 1807–1820, 1998.
- [4] L. P. Gradinarsky, J. Johansson, H. R. Bouma, H.-G. Scherneck, and G. Elgered, "Climate monitoring using GPS," *Phys. Chem. Earth*, vol. 27, pp. 225–340, 2002.
- [5] S. Gutman, S. Sahm, S. Benjamin, B. Schwartz, K. Holub, J. Stewart, and T. L. Smith, "Rapid retrieval and assimilation of ground based GPS precipitable water observations at the NOAA forecast systems laboratory: impact on weather forecasts," *J. Meteorol. Soc. Jpn*, vol. 82(1B), pp. 351–360, 2004.
- [6] G. Kopp, G. Lawrence, and G. Rottman, "The total irradiance monitor (TIM): Science results," *Sol. Phys.*, vol. 230, pp. 129–140, 2005.

- [7] J. L. Davis, T. A. Herring, I. I. Shapiro, A. E. E. Rogers, and G. Elgered, "Geodesy by radio interferometry: effects of atmospheric modelling errors on estimates of baseline length," *Radio Sci.*, vol. 20, pp. 1593–1607, 1985.
- [8] G. Elgered, "Tropospheric radio-path delay from ground based microwave radiometry," in *Atmospheric Remote Sensing by Microwave Radiometry* (M. Janssen, ed.), ch. 5, New York: Wiley & Sons, Inc., 1993.
- [9] T. R. Emardson and H. J. P. Derks, "On the relation between the wet delay and the integrated precipitable water vapour in the European atmosphere," *Meteorol. Appl.*, vol. 7, pp. 61–68, 2000.
- [10] J. Wang, L. Zhang, and A. Dai, "Global estimates of water-vapor-weighted mean temperature of the atmosphere for GPS applications," *J. Geophys. Res.*, vol. 110, 2005. doi: 10.1029/2005JD006215.
- [11] R. W. King, "Documentation for the GAMIT GPS analysis software." Internal report, 2002. <http://www-gpsg.mit.edu/~simon/gtgk/GAMIT.pdf>.
- [12] A. Niell, "Global mapping functions for the atmosphere delay at radio wavelengths," *J. Geophys. Res.*, vol. 101, no. B2, pp. 3227–3246, 1996.
- [13] K. Hocke, "Phase estimation with Lomb-Scargle periodogram method," *Ann. Geophys.*, vol. 16, pp. 356–358, 1998.
- [14] T. Emardson, J. Johansson, and G. Elgered, "The systematic behavior of water vapor estimates using four years of GPS observations," *IEEE Trans. Geosci. Remote Sens.*, vol. 38, pp. 324–329, January 2000.
- [15] R. Schmid and M. Rothacher, "Estimation of elevation-dependent satellite antenna phase center variations of GPS satellites," *J. Geod.*, vol. 77, no. 7–8, pp. 440–446, 2003.
- [16] C. G. Jones, U. Willén, A. Ullerstig, and U. Hansson, "The Rossby Centre regional atmospheric climate model part I: Model climatology and performance for the present climate over Europe," *Ambio*, vol. 33, no. 4–5, pp. 199–210, 2004.
- [17] E. Kjellström, L. Bärring, S. Gollvik, U. Hansson, C. Jones, P. Samuelsson, M. Rummukainen, A. Ullerstig, U. Willén, and K. Wyser, "A 140-year simulation of European climate with the new version of the Rossby Centre regional atmospheric climate model (RCA3)," Reports Meteorology and Climatology, 108, SMHI, SE-60176 Norrköping, Sweden, 2005. 54 pp.
- [18] S. M. Uppala, P. W. Kållberg, A. J. Simmons, U. Andrae, V. D. C. Bechtold, M. Fiorino, J. K. Gibson, J. Haseler, A. Hernandez, G. A. Kelly, X. Li, K. Onogi, S. Saarinen, N. Sokka, R. P. Allan, E. Andersson, K. Arpe, M. A. Balmaseda, A. C. M. Beljaars, L. V. D. Berg, J. Bidlot, N. Bormann, S. Caires, F. Chevallier, A. Dethof, M. Dragosavac, M. Fisher, M. Fuentes, S. Hagemann, E. Hólm, B. J. Hoskins, L. Isaksen, P. A. E. M. Janssen, R. Jenne, A. P. McNally, J.-F. Mahfouf, J.-J. Morcrette, N. A. Rayner, R. W. Saunders, P. Simon, A. Sterl, K. E. Trenberth, A. Untch, D. Vasiljevic, P. Viterbo, and J. Woollen, "The ERA-40 re-analysis," *Q. J. Roy. Meteorol. Soc.*, vol. 131, pp. 2961–3012, 2005.
- [19] N. van Lipzig, M. Schröder, S. Crewell, F. Ament, J.-P. Chaboureaud, U. Löhnert, V. Matthias, E. van Meijgaard, M. Quante, U. Willén, and W. Yen, "Model predicted low-level cloud parameters: Part I: Comparison with observations from the BALTEX bridge campaigns," *Atmos. Res. (Online)*, vol. 110, 2005. doi: 10.1016/j.atmosres.2006.01.010.